Sensors and Actuators B xxx (2014) xxx–xxx

Contents lists available at ScienceDirect

Sensors and Actuators B: Chemical

journal homepage: www.elsevier.com/locate/snb

A fast-response/recovery ZnO hierarchical nanostructure based gas sensor with ultra-high room-temperature output response

Xiaofang Pan [a], Xiaojin Zhao [a,b,**], Jiaqi Chen [a], Amine Bermak [a], Zhiyong Fan [a,*]

[a] Department of ECE, Hong Kong University of Science and Technology, Clear Water Bay, Hong Kong, PR China
[b] College of Electronic Science and Technology, Shenzhen University, Shenzhen, PR China

ARTICLE INFO

Article history:
Received 28 December 2013
Received in revised form 1 July 2014
Accepted 29 August 2014
Available online xxx

Keywords:
Hierarchical nanostructure
Room-temperature gas sensing
CMOS gas sensor

ABSTRACT

In this paper, a ZnO hierarchical nanostructure based gas sensor is presented. The proposed implementation features short response/recovery time and ultra-high output response at room temperature (RT). In order to take the advantages of complementary-metal-oxide-semiconductor (CMOS) process in terms of miniaturization and cost-effectiveness, a novel fabrication recipe, consisting of CMOS-compatible techniques, is proposed to form a patterned triple-layer metal, which functions as both interconnection electrodes and catalyst for our reported ZnO hierarchical nanostructure. This enables rapid and local growth of ZnO hierarchical nanostructure directly on a single silicon chip. Reported peak RT output response of 32 (20 ppm NO_2) provides a significant 28-fold improvement over the traditional widely adopted nanowire-based gas sensor. Meanwhile, a time efficient gas sensor is also validated by the presented temporal performance with a response and recovery time of 72 s and 69 s, respectively. In addition, compared with the previously demonstrated gas sensors operating at 200–300 °C, the proposed RT sensing completely removes the power-hungry heater and eliminates the related thermal reliability issues. Moreover, the demonstrated process flow well addresses the challenging issues of the traditional mainstream "drop-cast" method, including poor yield, non-uniformity of device performance and low efficiency caused by inevitable manual microscope inspection.

1. Introduction

In the past decade, nano-material and nano-structure based devices develop rapidly in the gas/chemical sensing area due to their exhibited extraordinary performance [1–5]. Attributed to its large surface to volume ratio [6,7], nano-scale dimension (close to Debye length) [8,9], and rich surface chemistry [10,11], nano-material with linear morphology (so-called "nanowire" (as shown in Fig. 1(a))) was first adopted and a number of nanowire-based implementations have been presented [10,12–16]. Despite the high output response reported for this nanowire structure, heating is still inevitable to maintain a high operating temperature (typically 200–300 °C) [17–22], resulting from the fact that the output response is closely correlated to the operating temperature. Consequently, with this classical nanowire structure, it is quite challenging to obtain a satisfactory response at room temperature (RT). The RT gas sensing is able to completely remove the needed power-hungry heater [23], and shows great promise to the gas sensor's monolithic integration with the complementary-metal-oxide-semiconductor (CMOS) analog/digital circuitries, which are typically operated at RT and thermally vulnerable [24]. This envisioned single-chip solution, featuring on-chip gas sensing/processing in real time, provides us a unique opportunity to take the advantages of low cost and continuing miniaturization of the standard CMOS process.

Additionally, we reported recently that at a temperature of 200 °C, ZnO hierarchical nanostructures (as shown in Fig. 1(b)) with non-linear morphology outperform the classical nanowire structure for their exclusive "self-gating" effect [25]. According to our theoretical modeling, it originates from the dendritic parts showing characteristic potential distribution after the surface chemical reaction with target gas molecules. In order to implement the promising gas sensing/processing system on a single chip, we further explored the ZnO hierarchical nanostructures RT gas sensing performance. Moreover, regarding the hierarchical nanostructures fabrication, several obstacles remain on the way to the aforesaid monolithic integration, including CMOS incompatibility [24], non-uniformity of device performance, and more significantly, extremely poor yield

* Corresponding author Tel:+852 2358 8027; fax: +852 2358 1485.
** Corresponding author at: College of Electronic Science and Technology, Shenzhen University, Shenzhen, PR China.
E-mail addresses: eexjzhao@szu.edu.cn (X. Zhao), eezfan@ust.hk (Z. Fan).

http://dx.doi.org/10.1016/j.snb.2014.08.089
0925-4005/

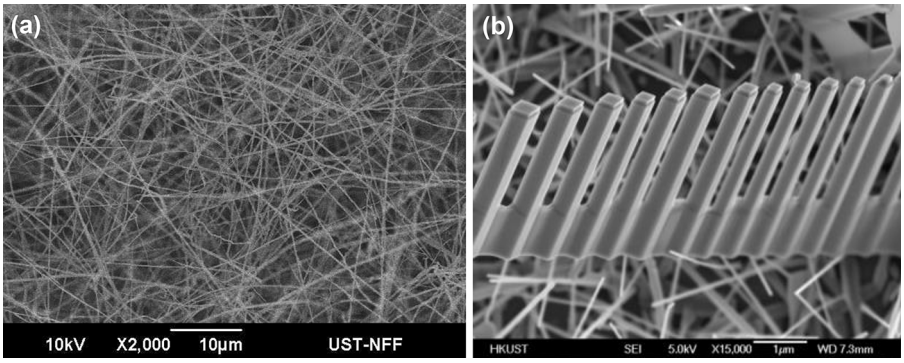

Fig. 1. (a) SEM image of nanowire, (b) zoomed SEM of hierarchical nanostructure.

of the fabricated nano-devices [26]. Generally, the most widely adopted approaches for fabricating nanostructure include chemical synthesis, ultrasonic exfoliation and transfer of the nano-devices onto the target silicon chip with pre-fabricated electrodes, namely "drop-cast" method [27]. This "drop-cast" method, as its name suggests, disperse the exfoliated nano-devices randomly on the silicon chip regardless of their contact quality with the metal electrodes, leading to very poor yield and uniformity. Furthermore, manual inspection with high-resolution microscope is always necessary to select a proper device, making the whole sensing system's mass production unrealistic [28].

In this paper, we report a novel high-yield fabrication approach for ZnO hierarchical nanostructures, which is quite suitable for mass production. The utilized process steps for patterning metal electrodes include standard photolithography, physical vapor deposition (i.e. evaporation) and lift-off, which are all fully CMOS-compatible. Gold catalyst contained in triple-layer metal electrodes is in turn exploited to realize the self-assembled growth of our customized ZnO hierarchical structures, leading to a dramatically improved device yield and uniformity. Furthermore, a case study of NO_2 sensing is chosen to validate our fabricated ZnO hierarchical nanostructure. Reported RT performance indicates that our proposed hierarchical nanostructure greatly outperforms traditional nanowire in terms of output response, response time and recovery time, which paves the way toward a cost-effective monolithic gas sensing/processing chip with ultra-lower power consumption. The remaining of this paper is organized as follows: Section 2 theoretically describes the sensing mechanism of the proposed ZnO hierarchical nanostructure; the detailed fabrication process flow is presented in Section 3; the experimental results are reported and compared with previous literatures in Section 4; the concluding remarks are provided in Section 5.

2. Sensing mechanism

ZnO is known as an n-type semiconductor for its dominant electrons contributed by the oxygen vacancy and Zn interstitial [29]. When exposed to oxidizing gas ambient (e.g. NO_2), the surface adsorbed NO_2 molecules captures electrons from the ZnO conduction band [30,31]. As a result, the induced surface depletion region is expanded and the overall resistance is increased. Based on this principle, traditional planar ZnO film was first utilized to make discrete electronic device for gas sensing applications. The planar ZnO film exhibits poor response due to its limited surface to volume ratio. For the large output response dependence on the operating temperature, heating was found to be an effective way to increase the response without considering the power consumption issue [32]. In order to take the advantage of the standard CMOS process's fast miniaturization trend, it is attractive to integrate the discrete ZnO film sensor on chip. The primary and most challenging issue is how to address the heating associated huge power consumption and meet the extremely limited on-chip power budget. ZnO nanowire based implementations were reported later to significantly improve the surface to volume ratio as well as the output response, which makes it possible to lower the required operating temperature and reduce the power needed for heating. Featuring nano-scale dimension close to the width of the surface depletion region, any change of the nanowire's surface depletion region width can cause much larger resistance variation, which corresponds to much higher output response. However, this improvement is still not enough to make the nanowire work properly with the operating temperature down to 25 °C (i.e. RT).

In this section, novel hierarchical nanostructures (Fig. 1(b)) are proposed to further extend the upper-limit of the response [25], especially the one at RT. As illustrated in Fig. 2(a), the proposed hierarchical nanostructure exhibits a unique morphology with "backbone" and "teeth" regions. Recently, we reported a "self-gating" effect based on the simulation of the internal electric field distribution of the hierarchical nanostructure [25]. Compared to the conventional nanobelt device with same dimension, shown in Fig. 2(c), it has been proven that that the conducting path at the "backbone" area can be manipulated by the "teeth" region, which results in a significantly improvement of gas sensing performance [25]. In addition, according to classical gas sensing mechanism and surface vacancy defect model [33,34], oxygen vacancy defects on the surface of the nanomaterial adsorb oxygen molecules of NO_2 and capture free electrons during this reaction. Meanwhile, these vacancy defects function as acceptors that reduce the free electron concentration and form electron depletion region at the surface (Fig. 2(d)). Specifically, it is found that a negative potential is formed between the source and the drain at the edge of the nanobelt surface (Fig. 2(d)). Moreover, the conduction path of this nanobelt device is narrowed due to the reaction between the NO_2 molecules and surface vacancy defects. As presented in Fig. 2(b), for the proposed hierarchical nanostructure, electrons are accumulated at the surface of "backbone" region as well as "teeth" region. Resulting from the nano-scale dimension, a huge potential drop can be formed at the "teeth" part. Consequently, the electric field distribution inside the "backbone" region is dramatically affected, which further narrows the aforesaid conduction path. In ref. 25, the simulation results have shown that the proposed hierarchical nanostructure's conductance differs from that of the nanobelt by one order of magnitude when exposed to the NO_2 gas. Furthermore, it is worth pointing out that the significant sensing performance improvement also attributed to its unique electron transport mechanism. Specifically, resulted from the surface trap states, the equivalent energy

Please cite this article in press as: X. Pan, et al., A fast-response/recovery ZnO hierarchical nanostructure based gas sensor with ultra-high room-temperature output response, Sens. Actuators B: Chem. (2014), http://dx.doi.org/10.1016/j.snb.2014.08.089

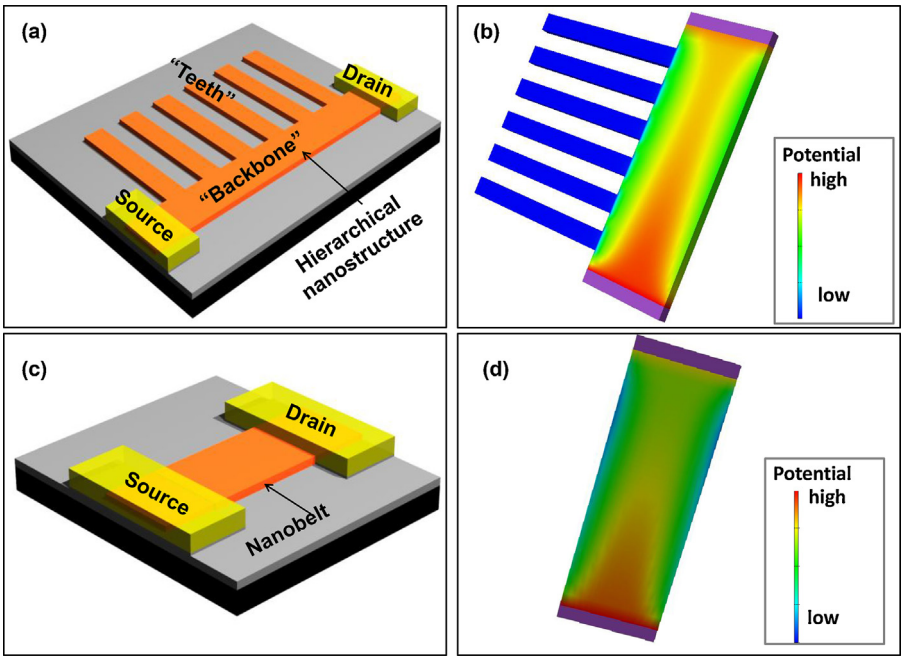

Fig. 2. (a) Proposed ZnO hierarchical nanostructure; (b) potential distribution of the proposed hierarchical nanostructure when exposed to NO_2 (generated by *Silvaco*); (c) traditional ZnO nanobelt; (d) potential distribution of the traditional nanobelt when exposed to NO_2 (generated by *Silvaco*).

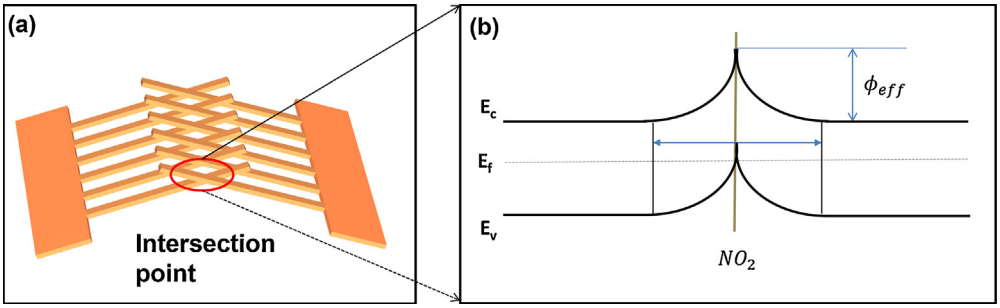

Fig. 3. (a) The illustration of the intersection point of the hierarchical nanostructure, (b) the energy band diagram after NO_2 adsorption.

band is bent at the ZnO nanostructure's surface [35]. When two or more nanostructures are connected as shown in Fig. 3(a), an energy barrier can be formed at each intersection point (Fig. 3(b)) [36]. Its influences on the transport of the electrons can be quantitatively expressed as follows [37,38]:

$$G = G_0 \exp\left(\frac{-\phi^{\text{eff}}}{k_B T}\right)$$

where ϕ^{eff} denotes the effective barrier height, k_B is the Boltzmann's constant, T is the absolute temperature and G is the conductance through the intersection point. In these equations, G_0 can be considered as a constant parameter. Typically, when exposed to NO_2, ϕ^{eff} is increased owning to the electrons trapped by the adsorbed oxygen molecules of NO_2. Therefore, the conductance G decreases exponentially with the increment of the energy barrier height. This leads to an efficient conducting path manipulation by the numerous energy barriers, which corresponds to a large number of the aforesaid nanostructure connections.

3. Fabrication

As the fabrication of ZnO nano-material based gas sensor, "drop-cast" method has been mainstream and widely exploited for years. However, mass production of devices is always hindered by several intrinsic issues existing in the "drop-cast" process flow, which can be summarized as follows:

(1) Ultrasonic exfoliation is usually the primary step to break down the grouped nanostructures and make them dissolved in some specific solution (e.g. IPA). Nevertheless, the inevitable ultrasonic force and wet solution corrosion can cause serious damages to the exfoliated nanostructures, which significantly reduce the devices' yield at the very beginning.
(2) The dissolved nanostructures are successively transferred onto the target substrate with the liquid solution drop, which typically forms a random nanostructure distribution. As a result, the contact quality with the pre-defined electrodes cannot be guaranteed and a manual inspection with high-resolution microscope is required to validate and select from numerous target devices. This time and labor consuming process further lowers the yield and makes the mass production prohibitive.
(3) Due to the process-caused non-uniform alignment orientation and contact resistance of single nanostructure, the chip-level variation of gas sensing performance makes it quite challenging to customize the on-chip analog readout, analog-to-digital (ADC) and digital processing circuitry. As a result, in order to address the non-uniformity issue, additional on-chip hardware

Please cite this article in press as: X. Pan, et al., A fast-response/recovery ZnO hierarchical nanostructure based gas sensor with ultra-high room-temperature output response, Sens. Actuators B: Chem. (2014), http://dx.doi.org/10.1016/j.snb.2014.08.089

overhead is necessary, such as the calibration module with complex calibration strategies.

To address the above issues, we propose a novel "solution-free" method to directly grow our ZnO hierarchical nanostructure between pre-defined metal electrodes, which fully avoids the ultrasonic-caused damage and the random distribution problem of nano-devices in the "drop-cast" method. With the top interconnection metal of standard CMOS process patterned as the aforesaid pre-defined metal electrodes, there is no extra silicon area dedicated to the added post-CMOS-process steps for our gas sensing nanostructure, causing only slight increment of the standard CMOS process's overall cost. After patterning the top interconnection metal, the standard CMOS process is finalized and the silicon chip with pre-defined metal electrodes is post-processed with gold layer evaporated on top as the catalyst of the nanostructure growth. This results in a self-assembled lateral growth of the ZnO nanostructure between adjacent metal electrodes toward each other. Compared with the "drop-cast" method, the proposed implementation forms the nanostructure locally and well preserves the hierarchical nanostructure's morphology. Meanwhile, it provides excellent self-assembly during the whole on-chip growth process and completely removes the need for transferring fragile nanostructures, both of which lead to significant improvement of the devices' yield.

In this section, we describe the detailed post-CMOS-process for fabricating our proposed ZnO hierarchical nanostructure. Specifically, a bare silicon wafer with silicon dioxide passivation layer is selected to mimic the uncut CMOS wafer with the top metallization finalized. A triple-layer sandwiched structure (i.e. Ti/Pt/Au) is then deposited and patterned on top. Among them, Au serves as the catalyst for ZnO growth, while Pt is utilized to form an ohmic contact with ZnO nano-device and Ti is selected to increase the adhesion with silicon substrate, respectively. It is worth to mention that the Pt and Ti layers can be eliminated with the uncut finalized CMOS wafer available. Additionally, vapor trapping chemical vapor deposition (CVD) is optimized to form specific ZnO nanostructure morphologies [39]. The vapor trapping CVD mainly consists of two steps: (1) Au nanoparticle catalyst saturation with vaporized Zn; (2) ZnO precipitation with the reactive oxygen gas. It is observed that the ratio between the vaporized Zn and the reactive oxygen gas is crucial to the nucleation process and the final morphology of ZnO nanostructures. Moreover, a vial is placed at the center of a quartz tube to create an environment with gradient Zn/O_2 vapor pressure. At the bunghole of the vial, the oxygen is relatively more concentrated, corresponding to a low zinc/oxygen pressure ratio. Therefore, by mounting the sample at the bunghole, ZnO is grown first anisotropically (usually in one dimension) then isotropically to form the presented "backbone" and "teeth" (Fig. 1(b)), resulting from a high nucleation rate and surface reaction rate [40,41]. In this way, ZnO hierarchical nanostructures with different morphologies can be produced and the detailed fabrication steps are summarized as follows:

(1) A bare silicon wafer with 1 μm pre-deposited silicon dioxide passivation layer is cleaned using deionized water for 4 cycles.
(2) A layer of photoresist (HPR 504) is spin-coated onto the aforesaid wafer at a speed of 4000 rpm for 30 s.
(3) After UV exposure with pre-designed mask and successive 60 s development in FHD-5 solution, the photoresist is patterned with the electrodes' region exposed.
(4) A sandwiched structure of Ti (20 nm)/Pt (80 nm)/Au (20 nm) is formed on the patterned photoresist by physical vapor deposition (i.e. evaporation).
(5) The whole wafer is then immersed in acetone to lift-off the metal outside the defined electrodes' region.
(6) The chip is then annealed at 700 °C for 30 min to form a layer of Au nanoparticles.
(7) 400 mg of Zn powder (99.9%, from Sigma–Aldrich Inc.) is placed at the bottom of the vial. Meanwhile, the substrate with patterned electrodes is mounted at the bunghole of the vial.
(8) After filling the tube with nitrogen, the furnace temperature is increased to 700 °C in 10 min. With the temperature exceeding the melting point of Zn (420 °C), Zn powder starts to vaporize and diffuse gradually toward the bunghole.
(9) Mixed gas of oxygen and argon (volume ratio: 1:49) is continuously injected into the furnace for 30 min under a pressure of 1 atm.
(10) Finally, the furnace is turned off and naturally cooled down to RT. With densely deposited ZnO nanostructures, the silicon wafer appears white.

4. Experimental results

In this section, we characterize the fabricated ZnO hierarchical nanostructures at RT. In order to facilitate the morphology and performance comparison, ZnO nanowires are fabricated with the same process flow and presented together with our proposed ZnO hierarchical nanostructures in Fig. 4, where the sensor electrodes are interdigitated with 10 μm distance between each other. The scanning electron microscope (SEM) pictures indicate that both nanowire and hierarchical nanostructures are selectively grown between the patterned electrodes. Moreover, the nanowires' diameter is measured to be around 400 nm (Fig. 1(a)) and the width of the hierarchical nanostructures' "backbone" is measured to range from several hundred nanometers to 1 μm (Figs. 1(b) and 4(a)). Furthermore, without the ultrasonic exfoliation, it is observed that the nanostructures group formation can be well preserved, which is completely different from the dissolved single nanostructure in the solution of "drop-cast" method. This significantly elevates the nanostructures' yield and improves the devices' reliability for the reason that the sensing result is averaged by large number of nanostructures, rather than a single nanostructure in the "drop-cast" method.

By exposing the fabricated devices to different concentrations of NO_2, the real-time resistance is continuously extracted and saved by our gas sensor test and characterization system shown in Fig. 5. We summarize the detailed measurement sequence as follows:

(1) The gas chamber is filled with N_2 to initiate the sample's resistance value, which is utilized as the reference baseline for the target gas to be sensed.
(2) A mass flow controller (MFC) is used to accurately monitor the target gas volume (i.e. NO_2) injected into the gas chamber in real time. With constant airflow velocity, the NO_2 concentration varies from 5 ppm to 20 ppm through filling NO_2 and N_2 combination having predetermined ratio.
(3) With the injection of different concentrations of NO_2, the sample starts to operate with the target gas concentration maintained until the sample's response curve saturates. The time interval between the start point and the saturation point is defined as the response time.
(4) Then N_2 is injected to reset the sample until the response curve restores the above-mentioned reference baseline. The time needed to restore the response curve from saturation to baseline is defined as the recovery time.
(5) In order to validate the stability and repeatability of test sample's performance, the above test sequence is repeated for multiple cycles.

Please cite this article in press as: X. Pan, et al., A fast-response/recovery ZnO hierarchical nanostructure based gas sensor with ultra-high room-temperature output response, Sens. Actuators B: Chem. (2014), http://dx.doi.org/10.1016/j.snb.2014.08.089

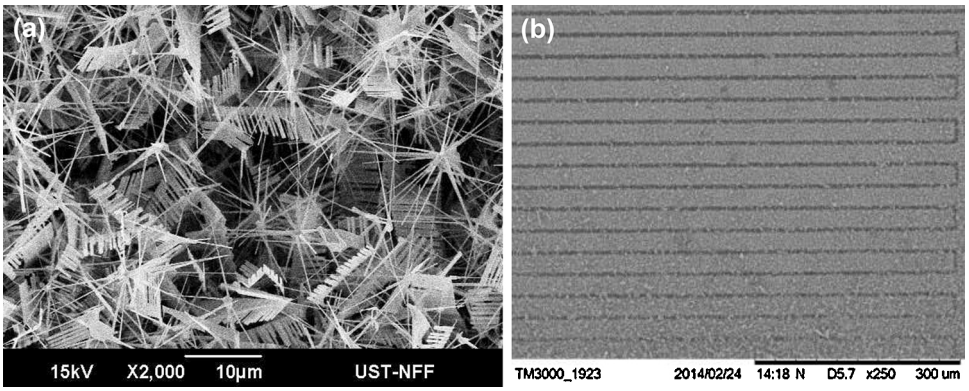

Fig. 4. (a) SEM image of hierarchical nanostructure, (b)interdigitated electrodes with hierarchical nanostructures grown on top.

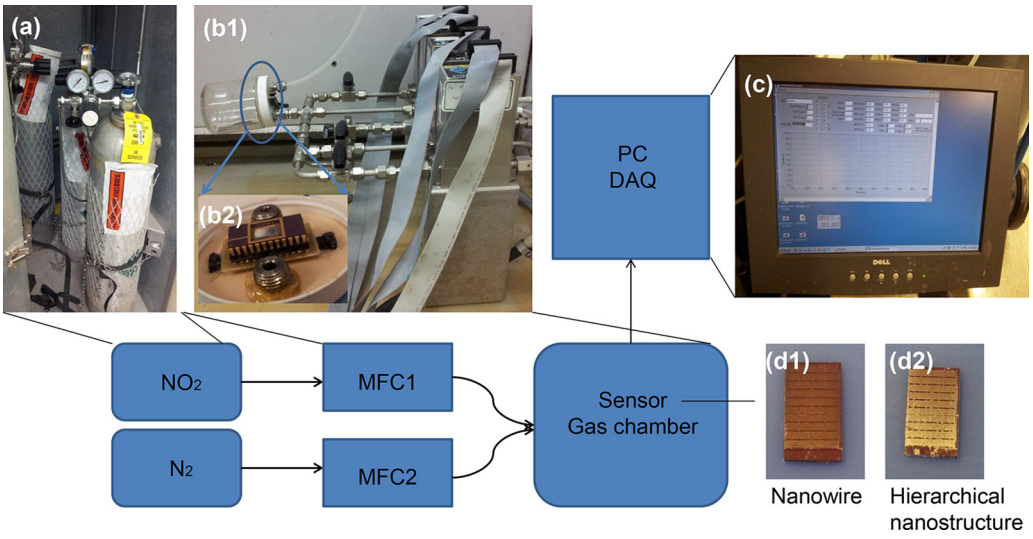

Fig. 5. Gas sensing measurement equipment, (a) the gas cylinders containing different gases, (b1) MFC and the gas chamber connected with it, (b2) the bonded chip for test, (c) the PC which controls the MFC, (d1) nanowire sample, (d2) hierarchical nanostructure sample.

Fig. 6 presents the temporal response of the ZnO hierarchical nanostructure exposed to 10 ppm NO_2, which shows excellent agreement with the sensing mechanism described in Section 2. Here the output response is defined as the ratio of the real-time measured resistance in target gas to that measured in N_2 (In order to exclusively reveal the sensing property of our fabricated sensor to the target gas, we chose N_2 as the recovering gas for its superior inertia to both types of reducing gas sensor and oxidizing gas sensor). Fast response and recovery are verified by the measured short response time and recovery time of 72 s and 69 s, respectively. For fair comparison, ZnO nanowire was also characterized with the same sequence as above-mentioned. Fig. 7 shows the temporal responses of both nanowire and hierarchical nanostructure samples, with the target gas concentration continuously varying from 5 ppm to 20 ppm (5 ppm step). In Fig. 7(a), the peak output responses of the nanowire test sample were measured to be 1.088, 1.105, 1.124 and 1.143 for NO_2 concentrations of 5 ppm, 10 ppm, 15 ppm and 20 ppm, respectively. The response time and recovery time were calculated to be 5 min and 10 min, respectively. In contrast, Fig. 7(b) indicates that the proposed hierarchical nanostructure based gas sensor significantly outperforms in all above-mentioned figures of merit. Specifically, as illustrated in Fig. 8(a), the peak responses were measured to be 12, 22, 27 and 32 for NO_2 concentrations of 5 ppm, 10 ppm, 15 ppm and 20 ppm, respectively, which exhibits a maximum improvement of 28-fold compared to its nanowire counterpart.

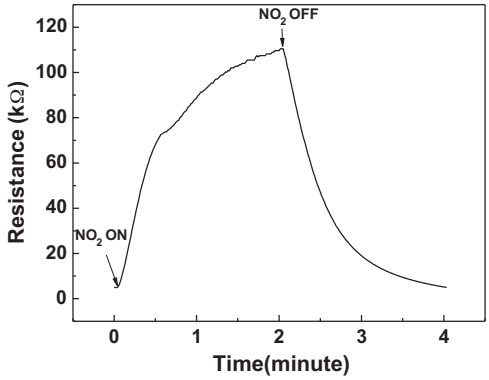

Fig. 6. Transient response of hierarchical nanostructure.

In order to further reveal the effectiveness of our proposed hierarchical nanostructure, we conduct a comprehensive comparison with all the related literatures and summarize the results in Table 1. In terms of response time, it is observed that the previously reported minimum is 10 min [42,43], which is 8 times slower than our proposed implementation. In addition, the reported peak responses for NO_2 concentration of 100 ppm is limited to 1.14–1.8 [42,43], which is much lower than our reported 32 for 20 ppm NO_2. As the recovery time, we take great advantage especially

Please cite this article in press as: X. Pan, et al., A fast-response/recovery ZnO hierarchical nanostructure based gas sensor with ultra-high room-temperature output response, Sens. Actuators B: Chem. (2014), http://dx.doi.org/10.1016/j.snb.2014.08.089

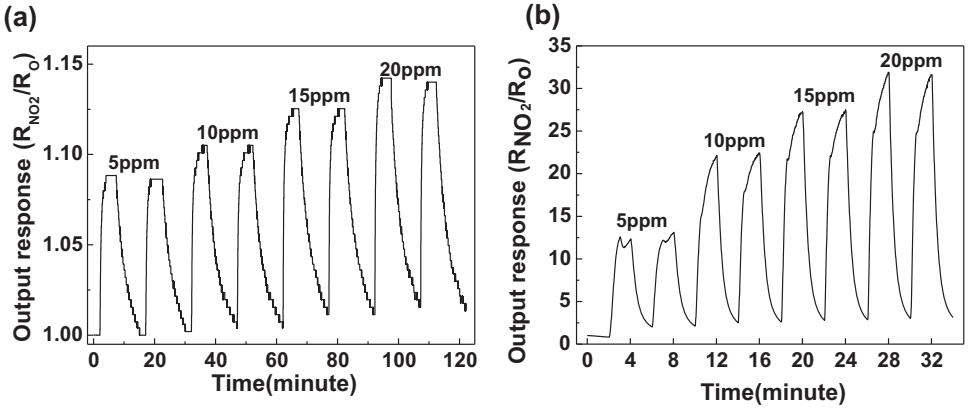

Fig. 7. (a) Sensing performance of nanowire based gas sensor at room temperature; (b) sensing performance of hierarchical nanostructure based gas sensor at room temperature.

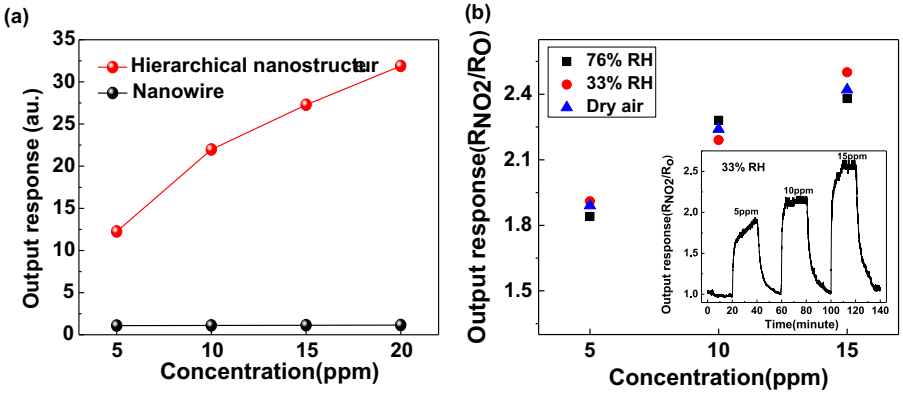

Fig. 8. (a) The relationship between output response and concentration using N_2 as the recovery gas; (b) The comparison between different humidity levels and dry air condition. The inset is the temporal response of 5 ppm, 10 ppm, 15 ppm NO_2 in the condition of 33% humid level.

compared to the reported ~120 min in Ref. [44]. Comparing the output responses against the previous implementation is difficult because this figure of merit is a function of gas concentration. As a result, it is very difficult to directly compare some of our results without access to the actual raw experimental results and without considering the target application. Nevertheless, we can observe that our proposed hierarchical nanostructure exhibits higher peak responses of 32 than the reported 1.14 [42], 1.8 [43], 6.7 [44] and 2.2 [45], under NO_2 concentrations higher or equal to 20 ppm. In Refs. [46–48], although it is hard to derive the peak responses of 20 ppm for fair comparison, the reported response time of 50–60 min and recovery time larger than 60 min make the real application too difficult.

We further extended our experiments to the reaction on NO_2 gas under the dry air and humid air environment (Fig. 8(b)). Accordingly, for 5 ppm, 10 ppm, 15 ppm, the output response is measured to be 1.86, 2.24, and 2.38 with the dry air as the recovery gas. It is observed that the sensor saturated within 20 min after the exposure to the target gas and recovered back to the baseline within 15 min. Due to the large volume of oxygen existing in the background environment (~21% in dry air), the output response and response/recover rate were degraded compared with the measurement results with N_2 as the recovering gas (Fig. 7(b)). However, compared with the reported responses by previous literatures at RT (Table 1), our fabricated sensor still has significant advantages over most of the reports in the table. Furthermore, it is worth mentioning that it takes over 100 min to recover for the sensors presented in Refs. [44,48], which makes their real applications too prohibitive. For Ref. [45], although exhibiting an output response close to this work, the demonstrated sensor requires a huge baseline resistance

Table 1
Room-temperature performance comparison with the previously reported NO_2 gas sensors.

Reference	Material	Output response	Response time	Recovery time	Recovery gas
[42]	TeO_2 thin film	1.14 for 100 ppm	10 min[a]	20 min[a]	Air
[43]	SnO_2 decorated CNT	~1.8 for 100 ppm	10 min[a]	>20 min[a]	Air
[44]	Double-heterojunction thin film	6.7 for 30 ppm[a]	~30 min[a]	~120 min[a]	Not reported
[45]	Nanopatterned polycrystalline ZnO	2.2 for 20 ppm[a]	15 min[a]	5 min[a]	Not reported
[46]	Graphene	0.7 for 5 ppm	60 min[a]	>60 min[a]	N_2
[47]	CNT/reduced graphene hybrid film	1.2 for 10 ppm	60 min	>60 min	N_2
[48]	InSb nanowire	1.04 for 4 ppm	50 min[a]	>100 min[a]	Air
This work	ZnO hierarchical nanostructure	32 for 20 ppm 2.5 for 20 ppm	72 s 20 min	69 s 15 min	N_2 Air

[a] Data deduced from the reported figure.

Please cite this article in press as: X. Pan, et al., A fast-response/recovery ZnO hierarchical nanostructure based gas sensor with ultra-high room-temperature output response, Sens. Actuators B: Chem. (2014), http://dx.doi.org/10.1016/j.snb.2014.08.089

(>45 GΩ), making its testing, calibration and real operation quite complicated. For the humidity level of 33% (the inset of Fig. 8(b)) and 76%, statistics of the measured output responses of NO_2 indicate a maximum standard deviation (SD) of 0.061 for the output response of 15 ppm NO_2, showing quite weak dependence on the humidity variations.

Additionally, the characterization of our fabricated hierarchical nanostructure is further extended to the reducing gas (H_2 and NH_3) and the vapors of common organic solvents (VOC). The measurement results of H_2 and NH_3 are summarized as follows:

(1) For H_2, output responses were neither observed at room temperature nor at 200 °C, which validates the superior selectivity of our fabricated gas sensor. This is consistent with the extensive experimental results reported in several previous Refs. [49–51,11].
(2) For NH_3, a slight resistance change was observed at the room temperature with long response and recovery time (72 min and 108 min, respectively). With large variation of NH_3 concentration (40 ppm → 80 ppm → 120 ppm), the corresponding output response, which is measured to be 0.808, 0.804 and 0.799, appears quite stable. This indicates that the sensor has been saturated with very limited variation of the sensing resistance.

According to the above experimental results, it is indicated that the sensor shows very limited response toward the reducing gas. This is partially due to the high baseline current, which is hard to be increased after the reaction with reducing gas. Therefore, this hierarchical nanostructure based gas sensor is more suitable for the oxidizing gas detection (e.g. NO_2) at room temperature.

What is more, we also conducted gas sensing test for our fabricated hierarchical nanostructure gas sensor with two typical VOC gases: benzene and formaldehyde. As a result, there is no obvious output response observed for both VOC gases neither at the room temperature nor at 200 °C. Regarding this, two possible reasons are provided as follows:

(1) For sensing the VOC gases, SMO may not be the first choice. As reported in the previous Refs. [52–54], polymer material exhibits better performance.
(2) The measured two VOC gases are categorized as reducing gas, which can increase the baseline current. However, the sensor's baseline current is already quite large and can be easily saturated, which is not suitable for the detection of reducing gas. Meanwhile, this shows excellent agreement with the aforesaid measurement results of NH_3.

5. Conclusions

In this paper, we report direct growth of ZnO hierarchical nanostructure between on-chip patterned electrodes. Compared with the mainstream "drop-cast" method, this "solution-free" method fully avoids the ultrasonic-caused damage and the nanostructures' random distribution. In addition, without the ultrasonic exfoliation, the nanostructures' group formation can be well preserved, which is completely different from the dissolved single nanostructure in the "drop-cast" method. This significantly elevates the nanostructures' yield and makes the sensing result close to the average of large number of nanostructures, not just a single nanostructure, leading to a much improved reliability. Moreover, the fabricated ZnO hierarchical nanostructures, operating at the RT, feature peak responses of 12, 22, 27 and 32 under NO_2 concentrations of 5 ppm, 10 ppm, 15 ppm and 20 ppm, respectively. With the response/recovery time around 70 s, the proposed implementation can find a wide range of applications requiring high-speed gas sensing/processing in real time and ultra-low power consumption.

Acknowledgements

This work was supported by RPC10EG20 from HKUST, Guangdong-Hong Kong Technology Cooperation Funding Scheme (project no. GHP/018/11SZ), Early Career Scheme 623112, Research Grant Council of Hong Kong, and Special Research Fund Initiative grants SRF11EG17-B and SRF11EG17PG-B from HKUST.

References

[1] J. Yi, J.M. Lee, W.I. Park, Vertically aligned ZnO nanorods and graphene hybrid architectures for high-sensitive flexible gas sensors, Sens. Actuators B 155 (2011) 264–269.
[2] S. Vallejos, T. Stoycheva, P. Umek, C. Navio, R. Snyders, C. Bittencourt, E. Llobet, C. Blackman, S. Moniz, X. Correig, Au nanoparticle-functionalised WO_3 nanoneedles and their application in high sensitivity gas sensor devices, Chem. Commun. 47 (2011) 565–567.
[3] B. Sun, J. Horvat, H.S. Kim, W. Kim, J. Ahn, G. Wang, Synthesis of mesoporous α-Fe_2O_3 nanostructures for highly sensitive gas sensors and high capacity anode materials in lithium ion batteries, J. Phys. Chem. C 114 (2010) 18753–18761.
[4] C.Y. Chen, M.W. Chen, J.J. Ke, C.A. Lin, J.R.D. Retamal, J.H. He, Surface effects on optical and electrical properties of ZnO nanostructures, Pure Appl. Chem. 82 (2010) 2055–2073.
[5] J.H. He, C.H. Ho, C.Y. Chen, Polymer functionalized ZnO nanobelts as oxygen sensors with a significant response enhancement, Nanotechnology 20 (2009) 065503.
[6] D. Li, J. Hu, R. Wu, J.G. Lu, Conductometric chemical sensor based on individual CuO nanowires, Nanotechnology 21 (2010) 485502.
[7] Y. Li, F.D. Valle, M. Simonnet, I. Yamada, J. Delaunay, High-performance UV detector made of ultra-long ZnO bridging nanowires, Nanotechnology 20 (2009) 045501.
[8] O. Lupan, V.V. Ursaki, G. Chai, L. Chow, G.A. Emelchenko, I.M. Tiginyanu, A.N. Gruzintsev, A.N. Redkin, Selective hydrogen gas nanosensor using individual ZnO nanowire with fast response at room temperature, Sens. Actuators B 144 (2010) 56–66.
[9] C.L. Zhu, Y.J. Chen, R.X. Wang, L.J. Wang, M.S. Cao, X.L. Shi, Synthesis and enhanced ethanol sensing properties of α-Fe_2O_3/ZnO heteronanostructures, Sens. Actuators B 140 (2009) 185–189.
[10] J. Du, D. Liang, H. Tang, X.P.A. Gao, InAs nanowire transistors as gas sensor and the response mechanism, Nano Lett. 9 (2009) 4348–4351.
[11] Y. Zhang, J. Xu, Q. Xiang, H. Li, Q. Pan, P. Xu, Brush-like hierarchical ZnO nanostructures: synthesis, photoluminescence and gas sensor properties, J. Phys. Chem. C 113 (2009) 3430–3435.
[12] E. Strelcov, Y. Lilach, A. Kolmakov, Gas sensor based on metal–insulator transition in VO_2 nanowire thermistor, Nano Lett. 9 (2009) 2322–2326.
[13] K. Skucha, Z. Fan, K. Jeon, A. Javey, B. Boser, Palladium/silicon nanowire Schottky barrier-based hydrogen sensors, Sens. Actuators B 145 (2010) 232–238.
[14] Z. Fan, J.G. Lu, Chemical sensing with ZnO nanowire field-effect transistor, IEEE Trans. Nanotechnol. 5 (2006) 393–396.
[15] Z. Fan, J.G. Lu, Gate-refreshable nanowire chemical sensors, Appl. Phys. Lett. 86 (2005) 123510.
[16] Z. Fan, D. Wang, P. Chang, W. Tseng, J.G. Lu, ZnO nanowire field-effect transistor and oxygen sensing property, Appl. Phys. Lett. 85 (2004) 5923.
[17] I.S. Hwang, E.B. Lee, S.J. Kim, J.K. Choi, J.H. Cha, H.J. Lee, B.K. Ju, J.H. Lee, Gas sensing properties of SnO_2 nanowires on micro-heater, Sens. Actuators B 154 (2011) 295–300.
[18] K.Y. Dong, J.K. Choi, I.S. Hwang, J.W. Lee, B.H. Kang, D.J. Ham, J.H. Lee, B.K. Ju, Enhanced H_2S sensing characteristics of Pt doped SnO_2 nanofibers sensors with micro heater, Sens. Actuators B 157 (2011) 154–161.
[19] S. Santra, P.K. Guha, S.Z. Ali, P. Hiralal, H.E. Unalan, J.A. Covington, G.A.J. Amaratunga, W.I. Milne, J.W. Gardner, F. Udrea, ZnO nanowires grown on SOI CMOS substrate for ethanol sensing, Sens. Actuators B 146 (2010) 559–565.
[20] X. Wang, Z. Xie, H. Huang, Z. Liu, D. Chen, G. Shen, Gas sensors, thermistor and photodetector based on ZnS nanowires, J. Mater. Chem. 22 (2012) 6845–6850.
[21] J. Chao, X. Xu, H. Huang, Z. Liu, B. Liang, X. Wang, S. Ran, D. Chen, G. Shen, Porous SnO_2 nanoflowers derived from tin sulfide precursors as high performance gas sensors, CrystEngComm 14 (2012) 6654–6658.
[22] B. Liu, J. Xu, S. Ran, Z. Wang, D. Chen, G. Shen, High-performance photodetectors, photocatalysts, and gas sensors based on polyol reflux synthesized porous ZnO nanosheets, CrystEngComm 14 (2012) 4582–4588.
[23] B. Guo, A. Bermak, P.C. Chan, G. Yan, An integrated surface micromachined convex microhotplate structure for tin oxide gas sensor array, IEEE Sens. J. 7 (2007) 1720–1726.
[24] J.W. Gardner, P.K. Guha, F. Udrea, J.A. Covington, CMOS interfacing for integrated gas sensors: a review, IEEE Sens. J. 10 (2010) 1833–1848.
[25] X. Pan, X. Liu, A. Bermak, Z. Fan, Self-gating effect induced large performance improvement of ZnO nanocomb gas sensors, ACS Nano 7 (2013) 9318–9324.

Please cite this article in press as: X. Pan, et al., A fast-response/recovery ZnO hierarchical nanostructure based gas sensor with ultra-high room-temperature output response, Sens. Actuators B: Chem. (2014), http://dx.doi.org/10.1016/j.snb.2014.08.089

[26] Y. Cui, M.T. Björk, J.A. Liddle, C. Sönnichsen, B. Boussert, A.P. Alivisatos, Integration of colloidal nanocrystals into lithographically patterned devices, Nano Lett. 4 (2004) 1093–1098.
[27] P. Chang, Z. Fan, W. Tseng, A. Rajagopal, J.G. Lu, β-Ga_2O_3 nanowires: synthesis, characterization, and p-channel field-effect transistor, Appl. Phys. Lett. 87 (2005) 222102.
[28] Y. Li, J.J. Delaunay, Progress toward nanowire device assembly technology, in: P. Prete (Ed.), Nanowires, 2010.
[29] S.B. Zhang, S.H. Wei, A. Zunger, Intrinsic n-type versus p-type doping asymmetry and the defect physics of ZnO, Phys. Rev. B 63 (2001) 075205.
[30] Z.P. Sun, L. Liu, L. Zhang, D.Z. Jia, Rapid synthesis of ZnO nano-rods by one-step, room-temperature, solid-state reaction and their gas-sensing properties, Nanotechnology 17 (2006) 2266.
[31] A. Kolmakov, Y. Zhang, G. Cheng, M. Moskovits, Detection of CO and O_2 using tin oxide nanowire sensors, Adv. Mater. 15 (2003) 997–1000.
[32] J.F. Chang, H.H. Kuo, I.C. Leu, M.H. Hon, The effects of thickness and operation temperature on ZnO:Al thin film CO gas sensor, Sens. Actuators B 84 (2002) 258–264.
[33] J. Ding, T.J. McAvoy, R.E. Cavicchi, S. Semancik, Surface state trapping models for SnO_2-based microhotplate sensors, Sens. Actuators B: Chem. 77 (2001) 597–613.
[34] J. Lagowski, E. Sproles, H. Gatos, Quantitative study of the charge transfer in chemisorption; oxygen chemisorption on ZnO, J. Appl. Phys. 48 (1977) 3566–3575.
[35] C. Soci, A. Zhang, B. Xiang, S.A. Dayeh, D.P.R. Aplin, J. Park, X.Y. Bao, Y.H. Lo, D. Wang, ZnO nanowire UV photodetectors with high internal gain, Nano Lett. 7 (2007) 1003–1009.
[36] Y.J. Choi, I.S. Hwang, J.G. Park, K.J. Choi, J.H. Park, J.H. Lee, Novel fabrication of an SnO_2 nanowire gas sensor with high sensitivity, Nanotechnology 19 (2008) 095508.
[37] Y. Chen, C. Zhu, X. Shi, M. Cao, H. Jin, The synthesis and selective gas sensing characteristics of SnO_2/α-Fe_2O_3 hierarchical nanostructures, Nanotechnology 19 (2008) 205603.
[38] T. Weis, R. Lipperheide, U. Wille, S. Brehme, Barrier-controlled carrier transport in microcrystalline semiconducting materials: description within a unified model, J. Appl. Phys. 92 (2002) 1411–1418.
[39] P.C. Chang, Z. Fan, D. Wang, W.Y. Tseng, W.A. Chiou, J. Hong, J.G. Lu, ZnO nanowires synthesized by vapor trapping CVD method, Chem. Mater. 16 (2004) 5133–5137.
[40] S.L. Mensah, V.K. Kayastha, Y.K. Yap, Selective growth of pure and long ZnO nanowires by controlled vapor concentration gradients, J. Phys. Chem. C 111 (2007) 16092–16095.
[41] J. Shi, H. Hong, Y. Ding, Y. Yang, F. Wang, W. Cai, X. Wang, Evolution of zinc oxide nanostructures through kinetics control, J. Mater. Chem. 21 (2011) 9000–9008.
[42] T. Siciliano, M.D. Giulio, M. Tepore, E. Filippo, G. Micocci, A. Tepore, Room temperature NO_2 sensing properties of reactively sputtered TeO_2 thin films, Sens. Actuators B 137 (2009) 644–648.
[43] G. Lu, L.E. Ocola, J. Chen, Room-temperature gas sensing based on electron transfer between discrete tin oxide nanocrystals and multiwalled carbon nanotubes, Adv. Mater. 21 (2009) 2487–2491.
[44] S. Ji, H. Wang, T. Wang, D. Yan, A high-performance room-temperature NO_2 sensor based on an ultra-thin heterojunction film, Adv. Mater. 25 (2013) 1755–1760.
[45] S.W. Fan, A.K. Srivastava, V.P. Dravid, Nanopatterned polycrystalline ZnO for room temperature gas sensing, Sens. Actuators B 144 (2010) 159–163.
[46] J.D. Fowler, M.J. Allen, V.C. Tung, Y. Yang, R.B. Kaner, B.H. Weiller, Practical chemical sensors from chemically derived graphene, ACS Nano 3 (2009) 301–306.
[47] H.Y. Jeong, D.S. Lee, H.K. Choi, D.H. Lee, J.E. Kim, J.Y. Lee, W.J. Lee, S.O. Kim, S.Y. Choi, Flexible room-temperature NO_2 gas sensors based on carbon nanotubes/reduced graphene hybrid films, Appl. Phys. Lett. 96 (2010) 213105.
[48] R.K. Paul, S. Badhulika, A. Mulchandani, Room temperature detection of NO_2 using InSb nanowire, Appl. Phys. Lett. 99 (2011) 033103.
[49] K. Kim, P. Cho, S. Kim, J. Lee, C. Kang, J. Kim, S. Yoon, The selective detection of C_2H_5OH using SnO_2-ZnO thin film gas sensors prepared by combinatorial solution deposition, Sens. Actuators B: Chem. 123 (2007) 318–324.
[50] N. Koshizaki, T. Oyama, Sensing characteristics of ZnO-based NO sensor, Sens. Actuators B: Chem. 66 (2000) 119–121.
[51] D. Zhang, S. Chava, C. Berven, S. Lee, R. Devitt, V. Katkanant, Experimental study of electrical properties of ZnO nanowire random networks for gas sensing and electronic devices, Appl. Phys. A 100 (2010) 145–150.
[52] A.D. Wilson, M. Baietto, Applications and advances in electronic-nose technologies, Sensors 9 (2009) 5099–5148.
[53] P. Si, J. Mortensen, A. Komolov, J. Denborg, P.J. Møller, Polymer coated quartz crystal microbalance sensors for detection of volatile organic compounds in gas mixtures, Anal. Chim. Acta 597 (2007) 223– 230.
[54] H. Bai, G. Shi, Gas sensors based on conducting polymers, Sensors 7 (2007) 267–307.

Biographies

Xiaofang Pan received her BS degree from Southeast University in Nanjing, China in 2010. She is currently pursuing her PhD degree in the Department of Electronic and Computer Engineering, the Hong Kong University of Science and Technology, Hong Kong. Her research activities are focused on nanomaterial and nanostructure functioned gas sensors for electronic nose applications.

Xiaojin Zhao received his BS degree from the Department of Microelectronics, Peking University in 2005 and PhD degree from the Hong Kong University of Science & Technology (HKUST) in 2010, respectively. After one year postdoctoral research work in HKUST, he joined the College of Electronic Science and Technology of Shenzhen University as an Assistant Professor. His research interests include CMOS monolithic polarization image sensor and gas sensor for the applications related to "Internet of Things".

Jiaqi Chen received his BS degree from Nanjing University in 2012. He is currently pursuing his PhD degree in the Department of Electronic and Computer Engineering, the Hong Kong University of Science and Technology, Hong Kong. His research interest focuses on gas sensing and testing.

Amine Bermak received the Master and PhD degrees, both in electrical and electronic engineering (microelectronics and Microsystems), from Paul Sabatier University, Toulouse, France in 1994 and 1998, respectively. In July 2002, he joined the Electronic and Computer Engineering Department of Hong Kong University of Science and Technology (HKUST), where he is currently a full Professor and ECE Associate Head for Research and Postgraduate studies. He has graduated 11 PhD and 14 MPhil students. He is a member of the IEEE Circuits and Systems Society committee on Sensory Systems as well as BIOCAS. He has served on the editorial board of IEEE Transactions on Very Large Scale Integration (VLSI) Systems and the Sensors Journal. He is also currently serving on the editorial board of IEEE Transactions on Biomedical Circuits and Systems; the Journal of Low Power Electronics and Applications, and Frontiers in Neuromorphic Engineering. He is the guest editor of the November 2010 special issue in IEEE Transactions on Biomedical Circuits and Systems. Prof. Bermak is a Fellow of IEEE and IEEE distinguished Lecturer.

Zhiyong Fan received his BS and MS degrees in physical electronics from Fudan University, Shanghai, China, in 1998 and 2001. He received his PhD degree from the University of California, Irvine, in 2006 in materials science. From 2007 to 2010 he worked in the University of California, Berkeley, as a postdoctoral fellow in the Department of Electrical Engineering and Computer Sciences, with a joint appointment with Lawrence Berkeley National Laboratory. In May 2010, he joined Hong Kong University of Science and Technology as an assistant professor. His research interests include engineering novel nanostructures with functional materials, for technological applications including energy conversation, electronics and sensors, etc.

Please cite this article in press as: X. Pan, et al., A fast-response/recovery ZnO hierarchical nanostructure based gas sensor with ultra-high room-temperature output response, Sens. Actuators B: Chem. (2014), http://dx.doi.org/10.1016/j.snb.2014.08.089